J Mater Sci (2008) 43:7179–7183
DOI 10.1007/s10853-008-3019-x

Structure evolution of bulk $Zr_{60}Cu_{20}Pd_{10}Al_{10}$ amorphous alloy during rolling deformation

P. N. Zhang · J. F. Li · Y. Hu · Y. H. Zhou

Received: 1 July 2007 / Accepted: 22 September 2008 / Published online: 23 October 2008

Abstract Bulk $Zr_{60}Cu_{20}Pd_{10}Al_{10}$ amorphous alloy was rolled at room temperature up to 96% reduction in thickness without fracture. The changes of microstructure and hardness during rolling deformation were investigated by X-ray diffraction, differential scanning calorimetry, high-resolution transmission electron microscopy, and microhardness measurement. It is revealed that the rolling deformation causes the quenched-in nuclei in the glass to grow slowly before a deformation degree of 90%. Substantial nanocrystallization occurs at higher deformation degree, where the softening induced by shear bands can even be compensated by the nanocrystallization.

Introduction

Bulk amorphous alloys have many unique properties, such as superior strength and hardness, excellent corrosion resistance, shaping and forming abilities in a viscous state, reduced sliding friction, improved wear resistance, and low magnetic energy loss [1, 2]. Amorphous alloys are metastable materials. Under the actions of external factors (e.g., mechanical force), their atoms may rearrange into new structure, revealed through molecular dynamics simulations by Murali et al. [3]. Therefore, it is important to examine the stability of the amorphous alloys against plastic deformation for their safe application.

P. N. Zhang · J. F. Li (✉) · Y. Hu · Y. H. Zhou
State Key Laboratory of Metal Matrix Composites, School of Materials Science and Engineering, Shanghai Jiao Tong University, Shanghai 200030, People's Republic of China
e-mail: jfli@sjtu.edu.cn

It is known that the plastic deformation of amorphous alloys is homogeneous at low stress and high temperature, but inhomogeneous at high stress and low temperature [4]. During inhomogeneous deformation shear bands with much free volume were introduced in the amorphous alloys, which enhance the disorder of the materials [5–9]. For example, Inoue [10] has noticed that when $Zr_{53}Ti_2Al_{10}Ni_5Cu_{30}$ amorphous alloy was rolled up to about 90% reduction in thickness, no appreciable fringe contrast region corresponding to crystalline phases could be seen in the deformed sample. On the other hand, the rise of the free volume content enhances the atomic diffusion, and nanocrystallization may be triggered. Plastic deformation-introduced nanocrystallization has been revealed in many amorphous alloys [11–14]. So far, it cannot be well predicted that an amorphous alloy will become more disordered or ordered during plastic deformation. Experimental investigation of the structural evolution of the amorphous alloy with deformation degree is still necessary. In the article, we present the microstructure and hardness changes induced by cold rolling in the bulk $Zr_{60}Cu_{20}Pd_{10}Al_{10}$ amorphous alloy.

Experimental

The master ingots were prepared by arc melting a mixture of pure Zr (99.9%), Cu (99.98%), Pd (99.99%), and Al (99.99%) metals under a Ti-gettered argon atmosphere. The ingot was inverted and remelted six times to ensure its compositional homogeneneity and then suck cast into a water-cooled Cu mold. The obtained plates were cut into specimens of 10 mm length, 2 mm width, and 1 mm thickness for rolling. The rolling apparatus consists of two rollers with a diameter of 100 mm. Covered by two steel plates with 1 mm original thickness, the specimen was

rolled repeatedly in one direction until the desired deformation degree was obtained. The deformation degree was denoted by the reduction in thickness $\varepsilon = (h_0 - h)/h_0$, where h_0 and h represented the specimen thickness before and after rolling, respectively. Many small deformation passes were used with a progressively narrowing gap between the two rollers. The decrease in the gap during deformation was carefully controlled so that the strain rate kept about 5.0×10^{-2} s^{-1}.

The structure of the specimen subjected to different deformation degrees was examined by X-ray diffraction (XRD) with monochromatic Cu-$K\alpha$ radiation. Thermal analyses of both the as-cast and the as-rolled specimens were performed in a Perkin–Elmer Pyris Diamond differential scanning calorimetry (DSC) instrument under a flow of purified argon. The heating rate is 20 K/min. A JEOL JEM-2100F high-resolution transmission electron microscopy instrument was used to examine the microstructures. The selected area electron diffraction (SAED) was performed on an area of 1 μm diameter. The microhardness of the specimen was measured by an HDX-1000 digital microhardness tester, which consisted of a square-based pyramidal diamond indenter with a 136° angle between two opposite faces. The static load was 100 g and the dwell time of loading was 15 s. Twenty indentations were made for each specimen.

Results

Thickness reduction as high as 96% was achieved during the rolling deformation. The specimen with such a high deformation degree has no cracks, and still exhibits a good ductility shown by a 180° bending without fracture. No crystalline phases were detected by XRD in the as-cast and as-rolled $Zr_{60}Cu_{20}Pd_{10}Al_{10}$ specimens, as shown in Fig. 1. By fitting the broad diffraction peak located at $2\theta \approx 38°$ using the Lorentz analysis, it becomes clear that the value of the full width at half-maximum (FWHM) increases by 5.2% from the as-cast to the rolled specimen with $\varepsilon = 90\%$ and then decreases by 1.4% from $\varepsilon = 90\%$ to $\varepsilon = 96\%$ (Fig. 2).

Figure 3 shows the DSC curves of the as-cast specimen and the rolled specimen. The crystallization takes place through two stages. When ε increased from 0 to 96%, both the peak temperatures of the first and second exothermic reactions, T_{P1} and T_{P2}, remain almost unchanged. Figure 4 shows the enthalpy of the two reactions, ΔH_1 and ΔH_2. ΔH_1 decreases slowly with the increasing in ε. An obvious decrease in ΔH_1 occurs in the range of ε from 90 to 96%. The magnitude is about by 1.9%. In contrast, ΔH_2 remains unchanged during deformation, which indicates that the rolling has no influence on the second crystallization event.

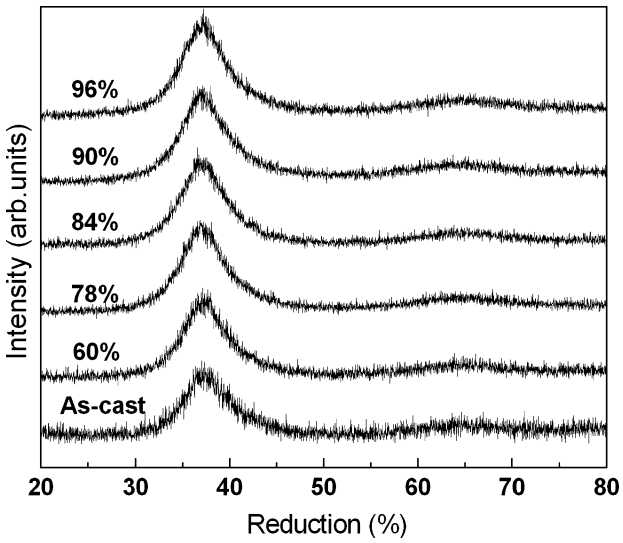

Fig. 1 Typical XRD patterns of the as-cast and rolled amorphous $Zr_{60}Cu_{20}Pd_{10}Al_{10}$ alloy

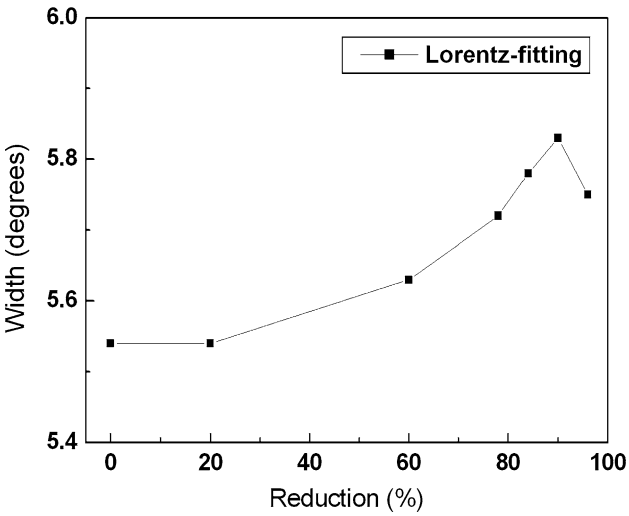

Fig. 2 FWHM of the amorphous $Zr_{60}Cu_{20}Pd_{10}Al_{10}$ alloy as a function of ε

Moreover, during rolling, the enthalpy at the glass transition (denoted as ΔH, calculated by integrating the heat flow between 500 and 670 K) was found to be reduced by 33% ($\varepsilon = 0$, $\Delta H = 4.02$ J/g; $\varepsilon = 90\%$, $\Delta H = 2.70$ J/g). This phenomenon was ascribed to the formation of nanovoids, which might lead to the reduction of the free volume [15].

The TEM images and SAED patterns of the as-cast specimen and the rolled specimen with thickness reduction of 96% are shown in Fig. 5. The bright-field TEM image of the as-cast specimen exhibits a uniform featureless contrast (Fig. 5a). The inset is the corresponding SAED pattern, in which no diffraction haloes or spots reflecting crystalline phases can be found. All these verify the amorphous nature

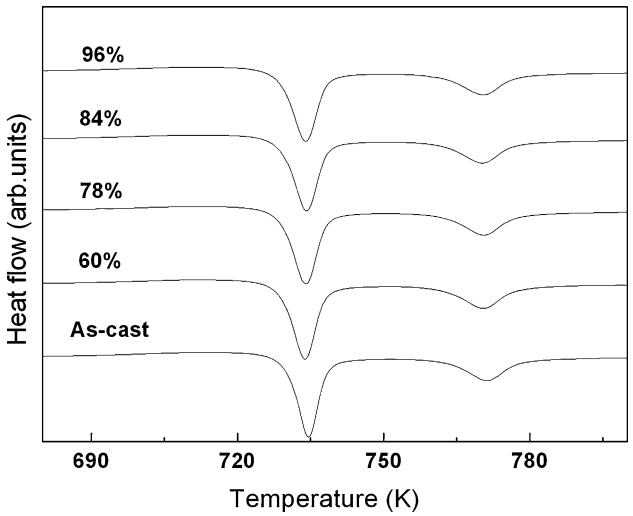

Fig. 3 DSC curves of the amorphous $Zr_{60}Cu_{20}Pd_{10}Al_{10}$ alloy

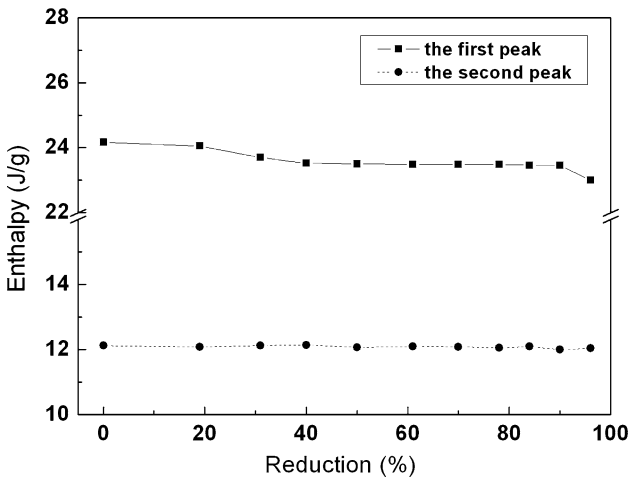

Fig. 4 The dependences of ΔH_1 and ΔH_2 on ε

of the as-cast specimen. Figure 5b shows the high magnification image of Fig. 5a, which is also amorphous. In the specimen rolled up to $\varepsilon = 96\%$, some dark precipitates appear in and around the shear band (Fig. 5c). In the SAED pattern diffuse rings originating from the amorphous matrix and some sharp diffraction rings and dots can be observed, indicating occurrence of nanocrystallization. Figure 5d shows the high magnification image of Fig. 5c, which possesses obvious lattice fringes. As the preparation process of all the TEM foils is strictly controlled, the possibility that the precipitates in the TEM foils result from the improper operation in preparation or the excessive radiation of the electron beam can be excluded. So the rolling at room temperature has induced nanocrystallization.

Figure 6 shows the microhardness at different reductions in thickness. It first decreases quickly from the as-cast value 5.65 to 4.86 GPa for $\varepsilon = 40\%$, and then decreases slowly in the range of $\varepsilon = 40\%$ to $\varepsilon = 90\%$. Beyond $\varepsilon = 90\%$, it increases from 4.82 to 5.00 GPa drastically.

Discussion

The amorphous $Zr_{60}Cu_{20}Pd_{10}Al_{10}$ alloy was rolled using multiple passes at a small amount of thickness reduction per pass, so as to get large reductions in thickness and minimize any thermal effect during deformation. When a metal is cold deformed, part of the mechanical energy is stored in the form of defects. For amorphous alloys, the consequence is an increase in the free volume in the shear bands, due to which FWHM constantly rises before $\varepsilon = 90\%$.

During inhomogeneous deformation the strain in the shear band is very high, while that in the areas far from the shear band is near zero. As preexisting shear bands are the weak links in the deformed amorphous alloys, as evidenced by the direct observation that they are preferentially etched [16] and exhibit different electron diffraction contrast from the undeformed material [17, 18], some shear bands may undergo repeated slippages during the subsequent deformation while new shear bands form. Correspondingly the microstructure change during rolling preferentially occurs inside or around the shear bands.

For the Zr–Cu–Pd–Al systems, the heat of mixing of Zr–Pd is −91 KJ/mol, being considerably more negative than those of the other atom pairs (the values of Al–Pd, Zr–Al, Zr–Cu, Cu–Pd, Cu–Al are −46, −44, −49, −14, −1 KJ/mol [19], respectively). Thus, Pd has strong attractive interaction with Zr. This may lead to the formation of short range order (Zr, Pd) domains in liquid state. When the liquid is cooled below the liquidus temperature, the size of the domains may further enlarge and finally the short-range order (Zr, Pd) rich domains remain as quenched-in nuclei in the amorphous phase [20]. It was reported that when the $Zr_{60}Cu_{20}Pd_{10}Al_{10}$ amorphous alloy was annealed near the glass transition temperature (T_g) or at higher temperatures, the Zr_2(Cu, Pd) nanocrystalline microstructure occurred [10]. The nanocrystallization was thought to be a result of a high density of quenched-in nuclei. The Zr–Pd atomic cluster seemed to act as preferential nucleation sites of Zr_2(Cu, Pd) phase. The subsequent growth reaction of the Zr_2(Cu, Pd) phase was sluggish because of the necessity of the redistribution of Al element into the remaining amorphous phase, the increase in the thermal stability of the remaining amorphous phase, and the enrichment of Al element at the amorphous/Zr_2(Cu, Pd) interface [21]. The growth of the quenched-in nuclei during deformation can be revealed by Fig. 4. The continuous decreasing of ΔH_1 shows the nuclei existed in the as-cast specimen grow as rolling deformation proceeds. A rapid growth of the nuclei

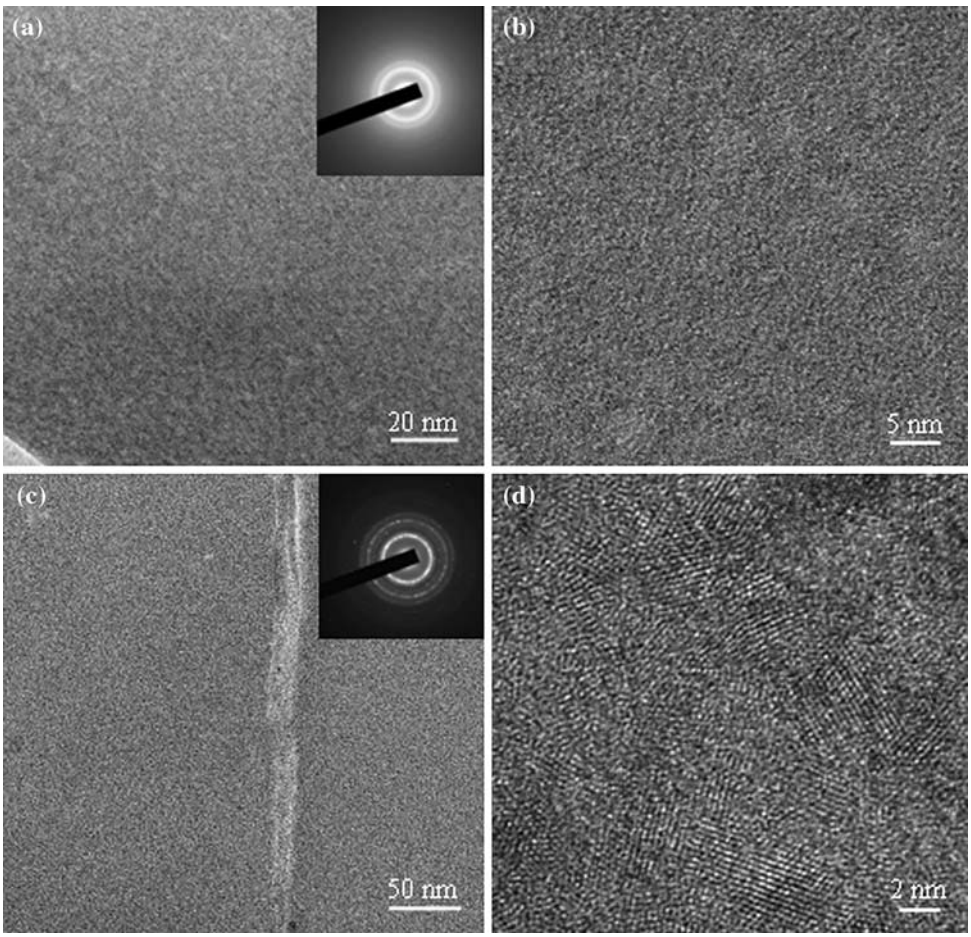

Fig. 5 TEM bright-field images and selected area diffraction patterns of the as-cast specimen (**a**), the rolled specimen with thickness reduction of 96% (**c**); **b** and **d** are the magnified TEM images of (**a**) and (**c**), respectively

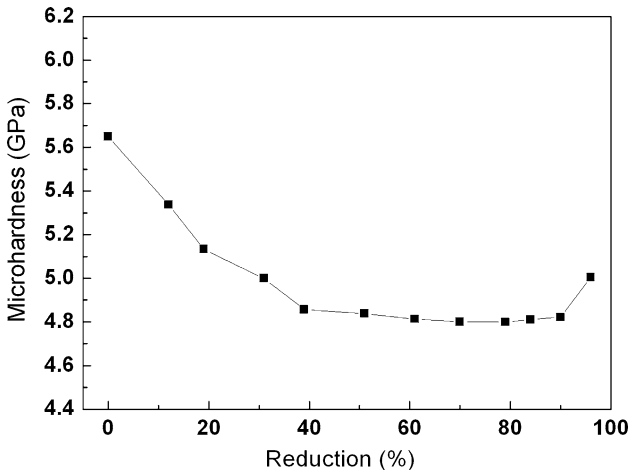

Fig. 6 Microhardness change with ε for the amorphous $Zr_{60}Cu_{20}Pd_{10}Al_{10}$ alloy

occurs at ε beyond 90%, thus nanocrystals with enough size to detect happened in the rolled specimen of $\varepsilon = 96\%$. Such a nanocrystallization even leads to an obvious decrease in the FWHM.

Inhomogeneous deformation is characterized by the formation of localized shear bands. The formation of shear bands in amorphous alloys must be associated with work softening behavior. The decrease in hardness from $\varepsilon = 0\%$ to $\varepsilon = 90\%$ can be contributed to the formation of the shear bands. On the other hand, nanocrystallites can often strengthen the amorphous matrix, as in nanocrystalline/amorphous matrix composites produced by thermal route [22–24]. The nanocrystallization induced by deformation makes the microhardness increase. The rise of the hardness when ε changes from 90 to 96% reflects that the nanocrystallization has been enough to compensate for the softening induced by shear bands.

Conclusions

The quenched-in nuclei in the $Zr_{60}Cu_{20}Pd_{10}Al_{10}$ amorphous alloy grow continuously during rolling deformation. However, the rise of free volume associated with shear bands formation dominates the structural and hardness changes before $\varepsilon = 90\%$. As a result, the FWHM constantly rises and the hardness decreases. As ε exceeds 90%, nanocrystallization substantially occurs, which makes the FWHM decrease and the hardness increase.

Acknowledgements Financial support from the National Natural Science Foundation of China under Grant No. 50671066 is acknowledged. The authors are grateful to Mr. Jianyi Tang and Ms. Hui Xing for the TEM observation.

References

1. Suzuki K, Kataoka N, Inoue A, Makino A, Masumoto T (1990) Mater Trans JIM 31:743
2. Yoshizawa Y, Oguma S, Yamaguchi K (1988) J Appl Phys 64: 6044
3. Murali P, Ramamurty U, Shenoy VB (2007) Phys Rev B 75: 024203
4. Schuh CA, Hufnagel TC, Ramamurty U (2007) Acta Mater 55: 4067
5. Jiang WH, Pinkerton FE, Atzmon M (2005) Acta Mater 53:3469
6. Jana S, Bhowmick R, Kawamura Y, Chattopadhyay K, Ramamurty U (2004) Intermetallics 12:1097
7. Spaepen F (1975) Acta Metall 23:615
8. Li J, Wang ZL, Hufnagel TC (2002) Phys Rev B 65:144201
9. Wright WJ, Hufnagel TC, Nix WD (2003) J Appl Phys 93:1432
10. Inoue A (1999) Bulk amorphous alloys: practical characteristics and application. Trans Tech Publications, Zurich, p 136
11. Jiang WH, Pinkerton FE, Atzmon M (2003) Scr Mater 48:1195
12. Kim JJ, Choi Y, Suresh S, Argon AS (2002) Science 295:654
13. Chen H, He Y, Shiflet GJ, Poom SJ (1994) Nature 367:541
14. Cao QP, Li JF, Zhou YH, Horsewell A, Jiang JZ (2006) Acta Mater 54:4373
15. Bhowmick R, Raghavan R, Chattopadhyay K, Ramamurty U (2006) Acta Mater 54:4221
16. Krishananand KD, Cahn RW (1975) Scr Metall 9:1259
17. Pampillo CA (1972) Scr Metall 6:915
18. Donovan PE, Stobbs WM (1981) Acta Metall 29:1419
19. Takeuchi A, Inoue A (2005) Mater Trans 46:2817
20. Fan C, Inoue A (2000) Appl Phys Lett 77:46
21. Inoue A, Fan C (1999) Nanostruct Mater 12:741
22. Kim YH, Inoue A, Masumoto T (1991) Mater Trans JIM 32:331
23. Sun WS, Quan MX (1996) Mater Lett 27:101
24. Kim HS (2003) Scr Mater 48:43